Using AI to Detect Climate Tipping Points- Or Why It's Hard to Understand Rapid Changes in the Earth System

Anand Gnanadesikan[1], G. Jay Brett[2], Jennifer Sleeman[2], David Chung[2]

[1]Morton K. Blaustein Department of Earth and Planetary Sciences Dept. Code P3901
The Johns Hopkins University, 3400 N. Charles St. Baltimore, MD 21218
[2]The Johns Hopkins University Applied Physics Laboratory
11100 Johns Hopkins Road, Laurel, MD 20723
gnanades@jhu.edu

Abstract

While rapid shifts in climate are seen throughout Earth's history, the dynamics which give rise to them are still obscured. This limits our ability to predict potential tipping points caused by human activity. In this paper, we discuss how Artificial Intelligence (AI) could be used to address the challenge of understanding tipping points by reducing the dimensionality of the Earth System, allowing for the isolation of key mechanisms and critically important parameters. We consider two examples of how AI might be used to examine such tipping points, one involving the ocean overturning circulation, the other involving ocean biogeochemical cycling.

Introduction

From the layering of rocks such as those seen in the Grand Canyon, to shifts in fossil assemblages within those layers, geologists have long realized that environments can change rapidly and irreversibly. As more work has been done on the history of atmospheric greenhouse gasses and orbital dynamics, it has become clear that such changes can occur as a result of relatively small variations in external forcing. For purposes of this paper we define such "tipping points" as occurring whenever some statistical property of the Earth System exhibits a disproportionate change as some threshold of forcing is passed. A number of these tipping points have occurred within the last 18,000 years as the Earth emerged from glaciation. The Younger Dryas, an approximately 1300-year period during which much of the Northern Hemisphere experienced a strong cooling, is thought to have been initiated over a period of less than 30 years (Severinghaus et al., 1998). Subsequent warming temperatures led to a greening of the Sahara Desert, which then reverted to a desert state about 5500 years ago (deMenocal et al., 2000). Over this same time period, there is evidence that the mode of tropical variability known as the El Niño-Southern Oscillation ceased, and then restarted (Carré et al., 2014). Understanding the vulnerability of the Earth System to such tipping points is made particularly urgent by the fact that the changes in forcing associated with increasing greenhouse gasses in the atmosphere are similar in magnitude to some of the forcings thought to have driven these recent tipping points.

Understanding these changes, however, is difficult. When it comes to the historical record, there are many indications that a particular change has happened, but not always indications of exactly when. For example, the disappearance of a species of tree from a region could be due to a change in mean wintertime temperatures, mean summertime aridity, increased climate variability or disease. Correlating changes on land to changes in the ocean is tricky because the primary way of dating oceanic proxies since the last glacial period (radiocarbon age) is offset from atmospheric radiocarbon ages by centuries, and this offset depends on circulation. This means that the direction of causality can be difficult to deduce.

An alternative approach is to use dynamical climate models. These models combine computational codes for simulating the evolution of atmosphere, ocean, cryosphere, and in some cases, the biosphere. "Dynamical cores" within these models divide each domain up into a grid, specify some "state variables" (i.e. sea surface height, temperature, and salinity in the ocean) and use these variables to construct a pressure field that varies in space. The resulting forces then drive velocities which redistribute the state variables and the system evolves in a self-consistent way. Biologically important variables like the concentration of oxygen or biomass of photosynthesizing organisms are transported by the resulting flows and have sources and sinks which can be mathematically codified. While such models are started

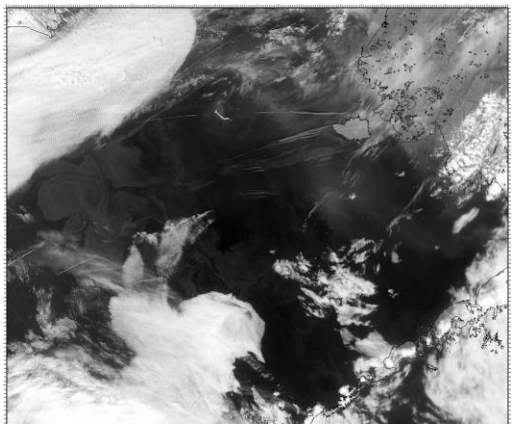

Figure 1: NASA image of clouds and phytoplankton over the Bering Sea. Image is about 1000 km on a side.

from modern conditions, they are generally spun up for hundreds to thousands of years to generate self-consistent estimates of the state of the Earth System. Tipping points are then sought by perturbing these quasi-equilibrium states by altering climate forcings such as greenhouse gasses.

A key shortcoming of such models is that critical climate processes occur over a vast range of scales, as illustrated by the image in Figure 1 which shows an ~1000x1000 km section of the Bering Sea. Both clouds in the atmosphere and blooms of plankton in the ocean show the imprint of processes on scales far smaller than the 100 km grid scale of most modern climate models. As a result, these processes must be "parameterized" in terms of state variables that can be simulated at coarse resolution. One of the simplest such parameterizations covers the impact of the eddies that create the impression of swirling cream in the figure as they advect and mix blooms of microscopic marine phytoplankton. The bulk impact of the mixing accomplished by such eddies is often represented as a lateral diffusion, where the flux of a quantity *C* is proportional to and down the gradient of the quantity (mathematically expressed as $F_C = -A_{Redi} \nabla * C$). As discussed in Abernathey et al. (2022), the value of the coefficient A_{Redi} is extremely uncertain and in the current generation of Earth System Models it varies from less than 200 m^2/s to 2000 m^2/s. Observational estimates run as high as 10000 m^2/s in some regions, but this may not matter if gradients are low there. The parameter A_{Redi} is only one of dozens of weakly constrained parameters- ranging from the number of cloud condensation nuclei over the ocean to the rooting depth of plants to the reflectivity of melting ice that contribute to the emergent behavior of climate models. Some of these may be important in setting a particular tipping point, while others are completely irrelevant.

As Earth System Models are constructed by coupling together models of individual component systems errors induced by incorrect values of one parameter or numerical schemes can be compensated by errors in other parameters or numerical schemes. As a result, the resulting codes represent both scientific and sociological compromises between the different groups of experts that contribute to the different components. Each group tries to make its own component as "realistic" as possible by including particular physics or biological processes (usually those of central interest to the model developer) and by focusing on particular metrics. However, this may result in compensating errors. For example, a high value of A_{Redi} may compensate the tendency of the jet stream to be located too close to the equator, resulting in a Gulf Stream that fails to penetrate far enough to the north.

Worse yet, these metrics may not all give the same results. For example, Gnanadesikan and Stouffer (2006) found that evaluating physical climate models based on whether they predicted the right terrestrial biomes gave a very different skill ranking than looking at the errors in temperature or precipitation alone. This was because the biome classification represents a nonlinear filter on temperature and precipitation: an overestimate of rainfall in the rainforest or underestimate of temperature in the tundra makes little difference in the predicted biome, while small errors at the edge of temperate regions can be much more important.

The metrics used by Earth System modelers to make judgements about how to represent key processes in the climate system are generally chosen to produce a "reasonable" simulation of the current climate when started from modern conditions and run for long periods of time. This raises the possibility that errors in one parameterization may be compensated by errors in others when the climate is close to its initial state, but that this compensation may not accurately capture tipping points when the model moves far from its initial state (Gnanadesikan, Kelson and Sten, 2018). But insofar as tipping points represent an emergent property of the climate system, how can we properly explore this question? And can AI methods help us to do so? In this manuscript, we present two examples of systems where we are exploring the use of AI methods to probe the nonlinear dynamics inherent in the Earth System, providing a means of interrogating the mechanisms within complex models.

Example 1: The ocean overturning circulation-dimensionality reduction as a way of exploring parameter sensitivity

Since the top few meters of the ocean hold as much thermal energy as the entire overlying atmosphere, changes in how the ocean circulates have the potential to redistribute large amounts of heat. One such circulation believed to have changed in the past is referred to as the Atlantic Meridional Overturning Circulation (AMOC). It is the result of a

complex pattern of currents whereby warm, salty tropical waters move northward in the Atlantic into the area around Greenland, where they lose heat, become dense, and sink. The heat flux associated with this circulation adds about 30-40 W/m^2 to the subpolar North Atlantic and Arctic Oceans, about half of ~85 W/m^2 added by absorbed sunlight (Yu, Jin and Weller, 2006). The overturning also plays an important role in setting the chemical structure of the ocean, as water moving away from the surface experiences a consumption of oxygen as organic material produced by phytoplankton falls into it and rots. The resulting apparent oxygen utilization (AOU) in the deep ocean (Figure 2) shows a clear global pattern, with local minima in the North Atlantic and Southern Ocean indicating that surface waters enter the deep ocean there, while a maximum in the North Pacific indicates that deep waters do not form there. However, in the modern generation of Earth System Models the overturning shows a wide range of mean values and sensitivities to global warming (Weijer et al., 2020; Romanou et al., 2023).

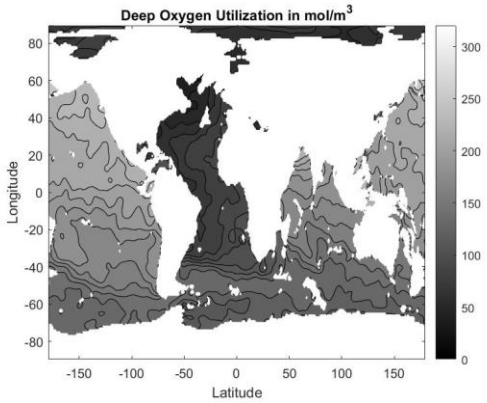

Figure 2: Oxygen utilization at 3000m. Low values in the North Atlantic indicate water has been in recent contact with the surface. Higher values moving in to the Indian and Pacific are the result of organic material falling into these waters and rotting, and broadly indicative of "age". Data taken from the World Ocean Atlas (Locarnini et al., 2019).

For decades it has been thought that the atmospheric water cycle shapes both the geometry and stability of the overturning circulation, (Johnson et al., (2019) provides a nice review of this). Net evaporation from the tropics and net precipitation in high latitudes drives the high latitudes to become fresh and light relative to the salty tropics. This tends to oppose sinking in polar regions. Within the Southern Ocean it actually results in transforming dense deep water to light water, balancing the cooling-induced sinking in the Northern Hemisphere (Gnanadesikan, 1999). Similarly, a net freshwater flux between the Atlantic and Pacific results in the Pacific becoming fresher and lighter. As the North Pacific becomes lighter than both the Southern Ocean and the North Atlantic, a positive feedback is triggered in which the export of salt associated with overturning to the deep drops, allowing the Pacific to become fresher and lighter and limiting overturning yet further. Similar feedback associated with meltwater coming off of North America remains the leading candidate to explain the Younger Dryas (Pico, Mitrovica and Mix 2020).

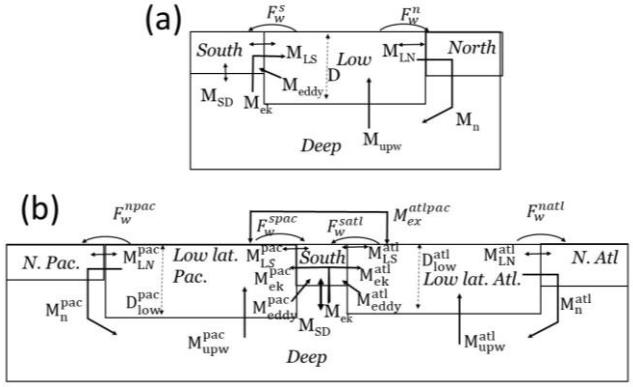

Figure 3: Schematic of (a) four box and (b) six box models of the ocean circulation. Curved lines show atmospheric freshwater fluxes while straight lines show mass exchanges between boxes.

These insights can be codified into so-called "box" models, which divide the ocean up into a finite number of well-mixed boxes. One example, described in Gnanadesikan, Kelson and Sten (2018), is shown in Figure 3a. In this model the ocean is broken down into a low-latitude box whose depth is allowed to increase as dense water is converted into light water (as we argue occurs in the Southern Ocean), and decrease as light water is converted into dense water (as occurs in the North Atlantic). Exchanges of water between boxes include a wind-driven upwelling of deep waters in the Southern Ocean (M_{ek}), a vertical exchange of water within the Southern Ocean associated with the formation of deep Antarctic waters (M_{sd}), turbulent exchanges between surface boxes (M_{LS}, M_{LN} governed by the eddy coefficient A_{Redi} previously referred to), an additional net mass transfer of light water into the Southern Ocean associated with turbulent eddies (M_{eddy}), upwelling of dense water into the low latitude surface boxes as heat is diffused downward (M_{upw}), and the conversion of light water to dense water in the North Atlantic associated with the AMOC (M_n) which is proportional to the density difference between the high northern and low latitude box and the square of the depth of the low-latitude box (D_{low}).

Each of these seven fluxes either represents or is associated with a free parameter which may vary between Earth System Models. There are five free parameters associated with geometry corresponding to choices about what areas are covered by the different boxes. There are eight free parameters associated with the fluxes of heat and moisture through the ocean surface corresponding to what

temperatures the surface boxes are restored to and how quickly this occurs plus two atmospheric fluxes of freshwater (F_w^n and F_w^s). Finally, there are nine initial conditions corresponding to the temperature and salinity in the four boxes plus the depth of the low-latitude box.

The original Gnanadesikan, Kelson and Sten (2018) paper focused on how the response of the overturning M_n to changes in the freshwater flux between the low-latitude and northern surface boxes F_w^n was modulated by A_{Redi} (which scales M_{LN} and M_{LS}) and similar scaling coefficients governing M_{eddy}, M_{upw} and M_n given present-day initial conditions. However it changed only one variable at a time. It is known that by changing combinations of parameters, initial conditions and boundary conditions we can generate simulations that predict very similar equilibrium temperatures and salinities, but which may have rather different overall stabilities. But how do we explore this multidimensional space?

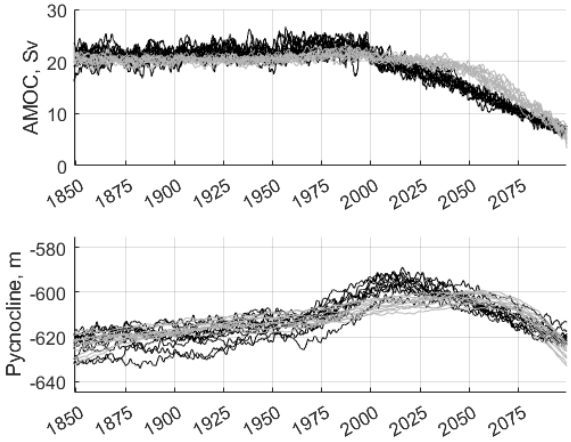

Figure 4: Top, AMOC overturning M_n in Sverdrups (1 Sv=10^6 m^3s^{-1}, slightly less than all the worlds rivers added together). Black from NCAR CESM2 Large Ensemble and gray from the fitted four-box model. Bottom, pycnocline depth in meters, with zero at the air-sea interface, same colors. All model output has a one-year moving mean applied.

One way to explore the space is to fit the box models to full general circulation models and evaluate whether the resulting models can predict changes in the overturning. Brett et al. (2023) demonstrate that this is feasible in theory. The box model in Figure 3a was fit to a flagship American climate model developed by the National Center for Atmospheric Research (NCAR CESM2, Danabasoglu et al., 2020). Monthly M_{ek}, M_{eddy}, M_n, F_w and density were derived from the first 11 ensemble members of the CESM2 large ensemble (Rodgers et al. 2021), which runs from 1850 to 2100 using historical and then SSP3-7.0 forcing for climate change. The parameters controlling M_{eddy}, M_{upw} were fitted using least-square errors for the first ensemble member. The four-box model was then run using derived fluxes (except M_n), densities, fitted parameters, and initial pycnocline depth. As shown in Figure 4, the model largely captures the evolution of the overturning and pycnocline depth, with mean correlation coefficients of 0.89 for M_n and 0.84 for D_{low}.

Additional work reported in Sleeman et al. (2022) has used this box model to train a novel implementation of a Generative Adversarial Network (GAN), known as TIP-GAN, to explore the parameter space. In this framework, generators vary initial conditions and parameters to turn the overturning off and a discriminator "learns" to predict which sets of parameters and initial conditions will return in overturning off or on. The result of this adversarial game is the shape of the manifold separating the different states. Figure 5 shows one result from the GAN, in which the initial depth of the pycnocline D_{low}, the Northern Hemisphere freshwater flux F_w^n and coefficient A_{Redi} are varied together. An interesting result from this figure is that by varying the initial conditions and eddy mixing coefficient together we can extend the "off" state to much lower levels of freshwater flux than if we vary only one of the parameters. This has implications for easily the overturning recovers from shutoff.

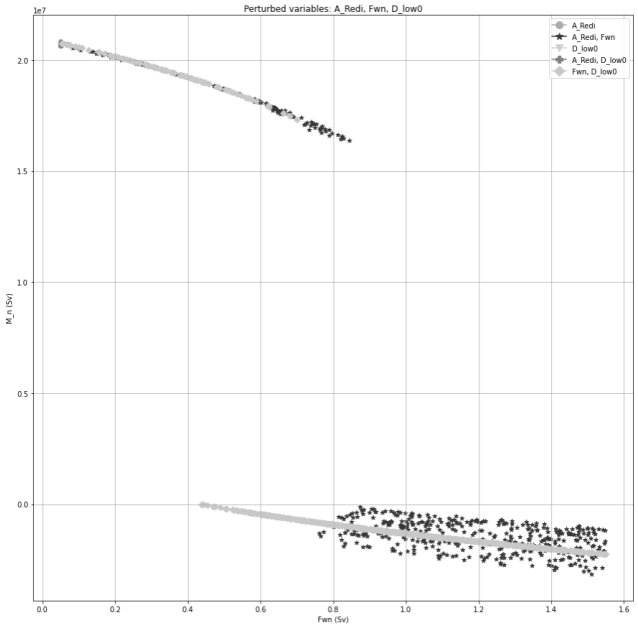

Figure 5. Predictions of the NH overturning in which northern hemisphere freshwater flux (horizontal axis) is varied. Upper branch of predictions shows "on" state, lower branch "off" state, which occurs when freshwater flux is strong enough to make the high northern latitude sufficiently light. Points show simulations in which the initial depth of the pycnocline D_{low} and the mixing coefficient A_{Redi} were varied separately.

Another early result of this work was the realization that the overturning was capable of switching off and then switching back on again, even when the forcing is constant. This behavior differs from that seen in the classic box model of Stommel (1961) which exhibits a fold bifurcation. We are currently exploring the reasons for this behavior. We are also extending this work to the six-box model shown in Figure 3b, which distinguishes between overturning in the Atlantic and Pacific. This model shows a rich phenomenology with collapses in overturning in the Atlantic capable of restarting overturning the in Pacific. We believe the GAN approach will be particularly useful is scoping out this model when we add stochastic forcing, allowing us to focus on the probability distribution of tipping near the separatrix.

.

Example 2: Ocean biological cycling-using machine learning to compare apparent relationships

Another example where AI methods may be of use is in examining the emergent behavior of ecosystems. As already noted, ecosystems represent nonlinear filters on physical climate. They tend to be very sensitive to whatever factor (light, nutrients, water, temperature) is limiting, but insensitive to factors that are not. This means that not all errors are equivalent- a frozen tundra that is too cold will be unproductive regardless of the size of the error, On the other hand in many systems, once plankton or plants have a surplus of one key nutrient, they will grow until they run out of another nutrient.

Many ecosystems, both terrestrial and marine, show clear linkages with climate. One such example is provided in Figure 6a, which shows the annual mean distribution of biomass of phytoplankton, which make up the base of the marine food web. High values are seen at both high and equatorial latitudes, while low values are found in the ocean interiors at latitudes between 20 and 40 degrees. The key controls on this distribution are well known. Phytoplankton need both light and nutrients, but as they are consumed the organic matter produced sinks away from the sunlit surface, so that there is a constant flow of nutrients to depth. High levels of biomass are found in regions where upwelling and mixing bring nutrient into surface waters, while low levels are found where surface waters converge.

Understanding the relationship between circulation and phytoplankton distribution, however, is challenging. Phytoplankton are extremely diverse, but the vast majority of them cannot be cultured in the laboratory, so that we do not understand their response to changes in different nutrients. Phytoplankton must make different tradeoffs to

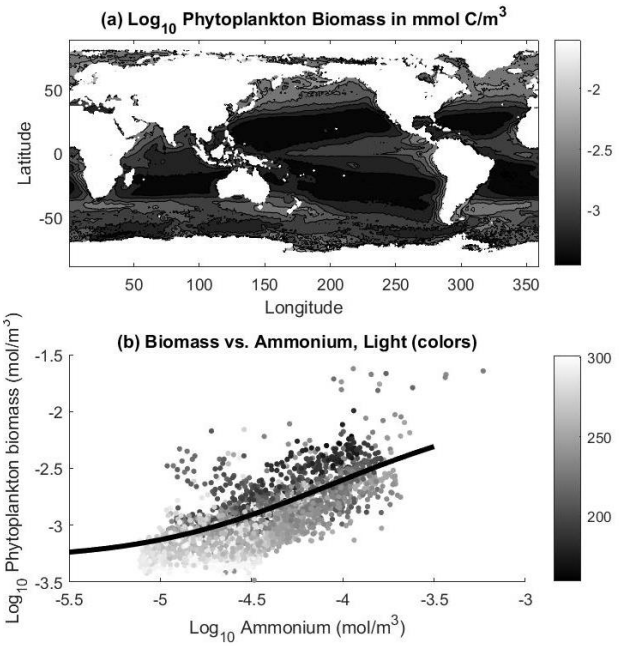

Figure 6: Phytoplankton biomass in the ocean. (a) $\log_{10}$ phytoplankton biomass in mol C/m^3 from the satellite dataset of Kostadinov et al. (2016). (b) Relationship between biomass and ammonium, a key nutrient for phytoplankton in the North Atlantic during the month of July. Colors show solar radiation in W/m^2. While a potential "tipping point" is seen when ammonium drops below 10^{-4} mol N/m^3 for high light, it is not seen for low light. Line shows a potential nonlinear relationship that relates biomass to environmental growth rate as described in the text

maximize growth on the one hand and minimize loss through sinking and predation on the other. On monthly timescales, however, the growth and loss are approximately in balance, as individual phytoplankton divide at rates of O(1/day) but total phytoplankton biomass may only see one or two doublings in a month (Behrenfeld, 2010). This means that on an ecosystem average, growth rates (μ) must approximately balance loss rates. Insofar as loss rates tend to be some function $F(B)$of phytoplankton biomass B this implies that

$$\mu \sim F(B) \rightarrow B \sim F^{-1}(\mu) \quad (1)$$

(see Dunne et al., 2005 for more discussion of this). Phytoplankton growth often has the general relationship with nutrient N $\mu \sim N/(K_N + N)$ (assuming that all other growth factors are available) and many models encode such a relationship for several phytoplankton groups. If F then takes the simple form $F = \lambda_0(B - B_{crit})/B_*$ where B_{crit} is a critical value below which the consumers of phytoplankton cannot grow we find a form

$$B \sim B_{crit} + \mu N/\big(\lambda_0(K_N + N)\big) * B_* \quad (2)$$

Figure 6b shows the relationship between one such nutrient (ammonium) and phytoplankton for the North Atlantic

during the month of July. While there is clearly structure to this plot, so that one can draw a line of the form shown in Equation (2) (black line) through the lower point cloud, the response to ammonium is clearly also mediated by how much light is supplied to the ecosystem (colors). There is some suggestion that in waters with more light, biomass might experience a tipping point as ammonium drops below 0.1 mmol/m^3. But in waters with less light (gray points) this effect of reducing ammonium is significantly attenuated.

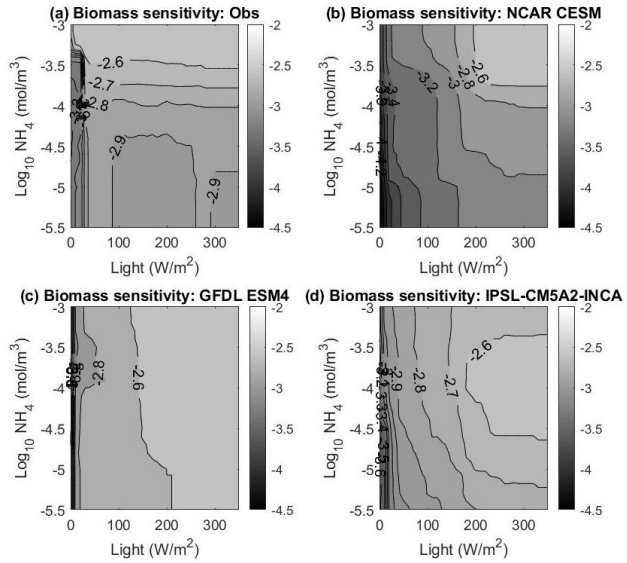

Figure 7: Sensitivity for the full domain of solar radiation and ammonium concentration with all other predictors held at median values. (a) Observational dataset of Kostadinov et al. (2016). (b) Same but for the NCAR CESM model (Danabasoglu et al., 2020). (c) Same but for the GFDL ESM4 (Dunne et al., 2020). (d) Same but for the IPSL-CM5A2-INCA model (Sepulchre et al.,2020)

AI methods have the potential to significantly improve our understanding of such systems (Holder and Gnanadesikan, forthcoming). By systematically examining the impact of individual environmental correlates with phytoplankton biomass, we can identify when and where tipping points might occur. We can also evaluate whether these apparent relationships are well-simulated by Earth System Models.

In Holder and Gnanadesikan (forthcoming), random forests (Breiman, 2001) were used to predict the log of phytoplankton biomass for observations and 13 Earth System Models. As discussed in this paper, the random forests turn out to predict a large fraction of the variability in our observational dataset (~90% of the observed variance in log biomass) and an even larger fraction in the models (>94%). In Figure 7 we examine what happens when median values of all predictors except ammonium and solar radiation are fed to the random forest. Qualitatively all of the plots show an increase in biomass as we move away from low levels of ammonium and radiation. However, differences appear in the overall dynamics. The observations (Figure 7a) show sharp drops, essentially tipping points, for both solar radiation and ammonium at low values of both light (-40 W/m^2) and ammonium (<5x10^{-3} mol/m^3). Similar analysis for three Earth System Models shows rather different patterns (Figure 7b-d). The NCAR CESM2 model (Figure 7b)-shows a very steep fall off at low light, but with a gradual increase in biomass as light increases out to over 200 W/m^2. A second flagship American Model, the Geophysical Fluid Dynamics Laboratory's Earth System Model 4 (GFDL ESM4, Figure 7c) shows relatively little dependence on ammonium and strong dependence on light. Finally, a flagship French model, the Institute Pierre et Simone Laplace's Coupled Model Version 5A2 (IPSL-CM5A2-INCA) shows a strong dependence on light, but limits the dependence on ammonium to high light cases, as opposed to the low-light dependence seen in the observations. While the reasons for this emergent behavior are not clear, it is obvious that AI methods can be used to predict differences in the conditions under which tipping points would occur. We are currently exploring whether these predictions from the random forest models explain inter-model differences in the response of phytoplankton biomass to global warming.

Conclusions

The great degree of complexity and nonlinearity in the Earth System might suggest that it is impossible to model tipping points in a system whose fundamental dynamics are poorly understood. This is supported by the wide divergence in the ability of Earth System Models to both simulate modern phenomena such as the global overturning circulation or the distribution of phytoplankton biomass and the divergence between such models in predicting future behavior of such phenomena under global warming.

However, as we have argued in this manuscript, AI methods may offer some pathways for reducing this uncertainty or at least identifying its sources. Both the overturning circulation and the distribution of ocean biomass give hints of being describable by systems with a much smaller number of degrees of freedom and associated parameters than the millions of individual boxes incorporated in a modern Earth System Model. Deploying machine learning/AI methods to both reduce dimensionality and identify key relationships and parameters offers us the ability to evaluate and improve models of the Earth System. However, this will only be the case if such methods are used with a focus on mechanistic understanding, rather than as black boxes to emulate more complex models.

Acknowledgments

Approved for public release; distribution is unlimited. This material is based upon work supported by the Defense Advanced Research Projects Agency (DARPA) under Agreement No. HR00112290032.

References

Abernathey, R; Gnanadesikan,A.; Pradal, M.A.; Sundermeyer, M.S. 2022 Isopycnal mixing, in Meredith, M. and A. Naviera-Garabato (eds.), Ocean Mixing-Drivers, Mechanisms and Impacts, 215-256 Elsevier. doi: 10.1016/B978-0-12-821512-8.00016-5.

Behrenfeld, M.J., 2010. Abandoning Sverdrup's critical depth hypothesis on phytoplankton blooms. Ecology, 91(4), pp.977-989, doi: 10.1890/09-1207.1.

Breiman, L.,2001. Random forests, Machine Learning, 45, 5–32, doi:10.1023/A:1010933404324.

Carré, M.; Sachs, J.P.; Purca, S.; Schauer, A.J.; Braconnot, P.; Falcón, R.A.; Julien, M.; Lavallée, D. 2014. Holocene history of ENSO variance and asymmetry in the eastern tropical Pacific. Science, 345,1045-1048., .doi:/ 0.1126/science.1252220

Danabasoglu, G.; Lamarque, J.-F.; Bacmeister J.; Bailey, D. A.; DuVivier, A. K.; Edwards, J.; Emmons, L. K.; Fasullo, J.; Garcia, R.; Gettelman, A.; Hannay, C.; Holland, M. M.; Large, W. G.; Lauritzen, P. H.; Lawrence, D. M.; Lenaerts, J. T. M.; Lindsay, K.; Lipscomb, W. H.; Mills, M. J.; Neale, R.; Oleson, K. W.; Otto-Bliesner, B.; Phillips, A. S.; Sacks, W.; Tilmes, S.; Kampenhout, L. van; Vertenstein, M.; Bertini, A.; Dennis, J.; Deser, C.; Fischer, C.; Fox-Kemper, B.; Kay, J. E.; Kinnison, D.; Kushner, P. J.; Larson, V. E.; Long, M. C.; Mickelson, S.; Moore, J. K.; Nienhouse, E.; Polvani, L.; Rasch, P. J.; and Strand, W. G. 2020. The Community Earth System Model Version 2 (CESM2). J. of Advances in Modeling Earth Systems, 12, e2019MS001916, doi:10.1029/2019MS001916.

deMenocal, P.; Ortiz, J; Guilderson, T; Adkins, J; Sarnthein,M.. Baker, L;M.Yarusinsky 2000, Abrupt onset and termination of the African Humid Period: Rapid climate responses to gradual insolation forcing, Quaternary Science Reviews, 19, 347–361, doi:10.1016/S0277-3791(99)00081-5.

Dunne, J.P.; Armstrong, R.A.; Gnanadesikan, A.; Sarmiento, J.L., 2005. Empirical and mechanistic models for the particle export ratio. Global Biogeochemical Cycles, 19(4), GB4026, doi: 10.1029/2004GB002390.

Dunne, J. P.; Horowitz, L. W.; Adcroft, A. J.; Ginoux, P.; Held, I. M.; John, J. G.; Krasting, J. P.; Malyshev, S.; Naik, V.; Paulot, F.; Shevliakova, E.; Stock, C. A.; Zadeh, N.; Balaji, V.; Blanton, C.; Dunne, K. A.; Dupuis, C.; Durachta, J.; Dussin; R., Gauthier, P. P. G.; Griffies, S. M.; Guo, H.; Hallberg, R. W.; Harrison, M.; He, J.; Hurlin, W.; McHugh, C.; Menzel, R.; Milly, P. C. D.; Nikonov, S.; Paynter, D. J.; Ploshay, J.; Radhakrishnan, A.; Rand, K.; Reichl, B. G.; Robinson, T.; Schwarzkopf, D. M.; Sentman, L. T.; Underwood, S.; Vahlenkamp, H.; Winton, M.; Wittenberg, A. T.; Wyman, B.; Zeng, Y.,;Zhao, M. 2020 The GFDL Earth System Model Version 4.1 (GFDL-ESM 4.1): Overall Coupled Model Description and Simulation Characteristics, J. Advances in Modeling. Earth Systems, 12, e2019MS002015, doi: 10.1029/2019MS002015.

Gnanadesikan, A 1999. A simple model for the structure of the oceanic pycnocline, Science, 283, 2077-2079, doi: 10.1126/science.283.5410.2077.

Gnanadesikan, A.; Kelson, R; Sten,M. 2018. Flux correction and overturning stability: Insights from a dynamical box model, Journal of Climate, 31, 9335-9350, doi:10.1175/JCLI-D-18-0388.1.

Gnanadesikan, A., and Stouffer, R. 2006. Diagnosing atmosphere-ocean general circulation model errors relevant to the terrestrial biosphere using the Köppen climate classification. Geophys. Res. Lett, 33, L22701, doi:10.1029/2006GL028098.

Holder, C. and A. Gnanadesikan, forthcoming, How well do Earth System Models capture apparent relationships between phytoplankton biomass and environmental variables? Global Biogeochemical Cycles.

Johnson, H. L.; Cessi, P.; Marshall, D. P.; Schloesser, F.; Spall, M. A. 2019. Recent contributions of theory to our understanding of the Atlantic Meridional Overturning Circulation. J. of Geophysical Research: Oceans, 124, 5376– 5399. doi: 10.1029/2019JC015330

Kostadinov, T. S.; Milutinović, S.; Marinov, I.; Cabré, A 2016. Carbon-based phytoplankton size classes retrieved via ocean color estimates of the particle size distribution, Ocean Sciences, 12, 561–575, doi:10.5194/os-12-561-2016.

Locarnini, R. A., Mishonov, A. V., Baranova, O. K., Boyer, T. P., Zweng, M. M., Garcia, H. E., Reagan, J. R., Seidov, D., Weathers, K. W., Paver, C. R., and Smolyar, I. V. 2019. World Ocean Atlas 2018, Volume 1: Temperature, https://www.ncei.noaa.gov/access/world-ocean-atlas-2018/bin/woa18.pl.(Retrieved 15 June 2021).

Pico, T.;Mitrovica, J.X.; Mix, A.C., 2020. Sea level fingerprinting of the Bering Strait flooding history detects the source of the Younger Dryas climate event. Science advances, 6(9), eaay2935. doi: 10.1126/sciadv. aay2935.

Rodgers, K. B.; Lee, S.-S;, Rosenbloom, N.; Timmermann, A.; Danabasoglu, G.; Deser, C.; Edwards, J.; Kim, J.-E.; Simpson, I. R.; Stein, K.; Stuecker, M. F.; Yamaguchi, R.; Bódai, T.; Chung, E.-S.; Huang, L.; Kim, W. M.; Lamarque J.-F.; Lombardozzi; D. L.; Wieder, W. R.,; Yeager, S. G. 2021. Ubiquity of human-induced changes in climate variability, Earth System Dynamics., 12, 1393–1411, doi:10.5194/esd-12-1393-2021.

Romanou A; Rind D; Jonas J; Miller R; Kelley M; Russell G; Orbe C; Nazarenko L; Latto R; Schmidt GA 2023. Stochastic Bifurcation of the North Atlantic Circulation Under A Mid-Range Future Climate Scenario With The NASA-GISS ModelE. Journal of Climate. doi.org/10.1175/JCLI-D-22-0536.1

Sepulchre, P.; Caubel, A.; Ladant, J.-B.; Bopp, L.; Boucher, O.; Braconnot, P.; Brockmann, P.; Cozic, A.; Donnadieu, Y.; Dufresne, J.-L.; Estella-Perez, V.; Ethé, C.; Fluteau, F.; Foujols, M.-A.; Gastineau, G.; Ghattas, J.; Hauglustaine, D.; Hourdin, F.; Kageyama, M.; Khodri, M.; Marti, O.; Meurdesoif, Y.; Mignot, J.; Sarr, A.-C.; Servonnat, J.; Swingedouw, D.; Szopa, S.; Tardif, D. 2020. IPSL-CM5A2 – an Earth system model designed for multi-millennial climate simulations, Geosci. Model Dev., 13, 3011–3053, doi:10.5194/gmd-13-3011-2020.

Severinghaus, J.P.; Sowers, T.; Brook, E.J.; Alley, R.B.; Bender, M.L., 1998. Timing of abrupt climate change at the end of the Younger Dryas interval from thermally fractionated gases in polar ice. Nature, 391(6663), 141-146, doi: 10.1038/34346.

Sleeman J; Chung D; Gnanadesikan A; Brett J; Kevrekidis Y; Hughes M; Haine T; Pradal MA; Gelderloos R; Ashcraft C; Tang C. A 2023. Generative Adversarial Network for Climate Tipping Point Discovery (TIP-GAN). arXiv preprint arXiv:2302.10274.

Sleeman, J; Chung, D; Ashcraft, C; Brett, J.; Gnanadesikan, A; Kevrekidis, Y; Hughes, M; Haine, T; Pradal, MA; Gelderloos, R; Tang, C; Saxsena, A; White L 2023. "Using Artificial Intelligence to aid Scientific Discovery of Climate Tipping Points. arXiv preprint arXiv:2302.06852.

Stommel, H., 1961. Thermohaline convection with two stable regimes of flow. Tellus, 13(2), pp.224-230. doi: 10.1111/j.2153-3490.1961. tb00079.x

Weijer, W.; Cheng, W.; Garuba, O. A.; Hu, A.; Nadiga, B. T.; 2020. CMIP6 models predict significant 21st century decline of the Atlantic Meridional Overturning Circulation.Geophysical Research Letters, 47, e2019GL086075. doi: 10.1029/2019GL086075.

Yu, L.; Jin, X.; Weller, R. A. 2006. Objectively Analyzed Air-Sea Fluxes (OAFlux) For Global Oceans, Research Data Archive at the National Center for Atmospheric Research, Computational and Information Systems Laboratory, doi:10.5065/0JDQ-FP94.